Integration of Polymerase Chain Reaction in a Magnetoresistive Biochip

Mariana Soares Martins Antunes

Thesis to obtain the Master of Science Degree in Bioengineering and Nanosystems
Instituto Superior Técnico, Av. Rovisco Pais, 1049-001 Lisboa, Portugal

Article Info

Keywords:
Polymerase Chain Reaction
Magnetoresistive Biochip
Spin Valve Sensors
Portable Platform
Thermo Cycling Control
Integration

Abstract

Nanotechnology and microfabrication have emerged as powerful methods that promise exciting and integrated solutions for miniaturization and integration of sample processing, assay performance, nucleic acid amplification and analyte detection systems. The lab-on-a-chip (LOC) solutions have become an opportunity to bring accurate and sensitive point of care diagnostic tests and monitoring platforms. The disposability, sensitivity, cost-effectiveness, user-friendliness, small volume analysis and portability are the main advantages of these LOC systems. Polymerase chain reaction (PCR) assays on chip have been extensively applied for the diagnosis and monitoring of molecular genetic and infectious diseases. For the improvement of biochip microfabrication, a recent research of different substrates materials, passivation layer optimization and architecture designs have been reported. The calibration of magnetoresistive (MR) sensors as temperatures sensors have been studied in order to evaluate the system thermal parameters and ensure a temperature cycling system required for an optimal PCR reaction. A Pulse Width Modulation has been also developed to assure the sensors calibration, the thermal control, promoting a fast and accurate thermal response and very low power consumption. The integration of a PCR in a MR biochip controlled by a portable platform has been intensively investigated and has emerged as a motivating challenge for improvement of point of care and LOC applications in the nanotechnology world.

1 Introduction

Nanotechnology and microfluidic have emerged as powerful tools in the lab-on-a-chip (LOC) platforms development for diseases diagnosis and monitoring, which has been crucial the evaluation and improvement of global health in both developed and developing countries [1,2]. These platforms have been essential components for correctly detecting of disease as well as the treatment monitoring, both at individually or population level, limiting its spread and regulating the respective treatment[3]. Nowadays the nucleic acid analysis techniques have revealed a major impact in genome mapping, sequencing and high throughput antigen screening and the molecular disease biomarkers detection and monitoring[4]. LOC devices have revealed a major impact in a variety of fields of life sciences, such as, the genotyping of individuals, environmental sensing and monitoring, food quality management, forensic sciences, controlling of epidemic diseases, clinical diagnostic including molecular detection of hereditary and infectious disease[4-7]. Recently, the research and

development of diagnosis and monitoring platforms has integrated a powerful technique for deoxyribonucleic acid (DNA) amplification, polymerase chain reaction (PCR) on chip. Biochips miniaturization has enabled to achieve several benefits such as analysis time minimization, reagent consumption reduction and minimization of risk of sample contamination and often enhance of assays performance[8-12]. In this paper, we present a portable platform combining the PCR, which will used on the specific detection of gene mutations and DNA biomarkers related to cancer, or messenger ribonucleic acid (mRNA) in the case of virus detection with the high sensitivity, rapidity, and low cost of the magnetoresistive (MR) biochip.

1.1.1 Magnetoresistive Sensors

Magnetoresistance is the property of a material exhibits a change in electrical resistance in presence of an external magnetic field [13,14]. The magnetoresistive (MR) sensors integrated in biochip consist in spin valves (SV), which working mechanism is base on Giant Magnetoresistance (GMR). GMR sensors have become a potential element integrated in magnetic biosensors for detection or identification of biomolecules due to their good sensitivity to small magnetic fields, high signal to noise ratio and their simplified fabrication process [14,15]. In the biosensors applications, magnetic particles are used as markers of target biomolecules and the GMR elements detect the presence of the particles that are immobilized to the sensors through intermolecular interactions, DNA hybridization [16,17]. A transfer curve of a spin valve used in the biochip is shown in Figure 1-1 with a resistance between 800Ω and 900Ω and a MR of 7%. U-shaped SV sensor, which constitute the biochip core, was deposited in a Nordiko 3000 onto a glass substrate with the following structure: Ta 20Å /$Ni_{80}Fe_{20}$36Å /$Co_{81}Fe_{19}$23Å/Cu25Å/$Co_{81}Fe_{19}$23Å/$Mn_{76}Ir_{24}$80Å/Ta30 Å/$Ti_{10}W_{90}$(N) 150Å. Surrounding each sensor, the U-shaped current line was designed to enable the sample heating and subsequent the focusing of the particles onto the sensing area (Figure 1-1).

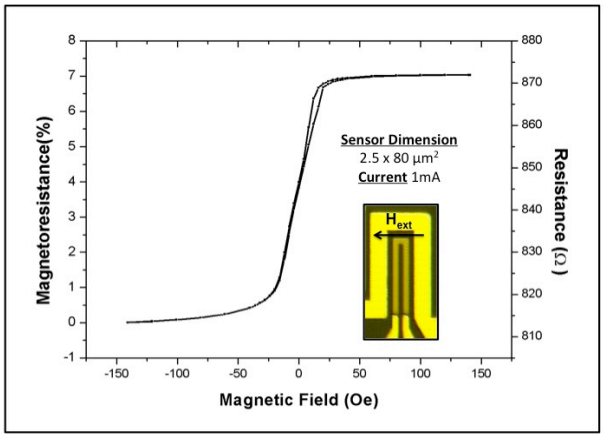

Figure 1-1: Typical transfer curve of a SV taken at a bias current of 1mA. The image shows the U-shaped 2.5x80µm^2 and a U-shaped current line surrounding the spin valve that is used for sample heating.

The biochip was designed with 6 different hybridization areas, each one with 5 SV used for temperature and magnetic detection (Figure 1-2). In each area, the 5 sensors were disposed in one column, and one of these is a reference sensor (SV without biologically active area).

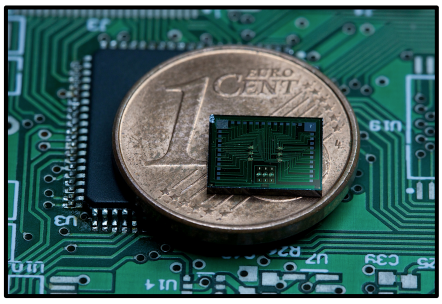

Figure 1-2: Biochip design with 6 different hybridization areas, each one with 5 sensors disposed in one column and one of these is a reference sensor.

The biochip platform used in this project, shown in Figure 1-3, includes all hardware components that are required to perform temperature control, real time signal processing and PCR on chip ensuring its portability[13,17]. The platform is also provided with a battery, which guarantees power and portability to the system. The platform is also provided with

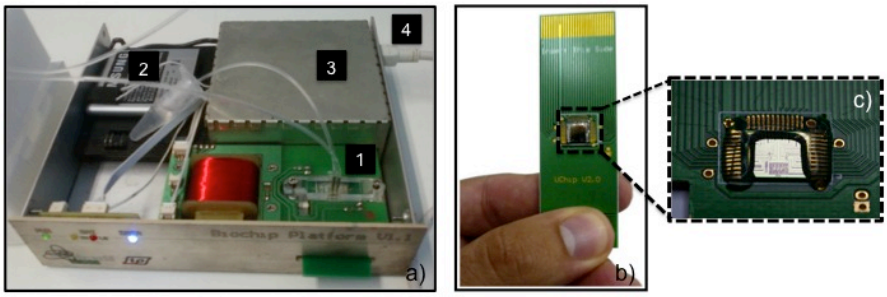

Figure 1-3: Topview of the portable platform for biological assays using a magnetoresistive biochip: a) 1) Biochip encapsulated in a PCB chip carrier with microfluidic platform 2) Battery 3) Acquisition and control board (the PCBs are placed inside this box) 4) USB connector; b) and c) Biochip encapsulated in a PCB chip carrier.

microfluidic module that consists of two different polymers: polymethylsiloxane (PDMS) and polymethilmethacrylate (PMMA) Due to its biocompatibility, its price and fast casting techniques, the PDMS was chosen to fabricate the U-shaped channel, and PMMA was used to fabricate the holder. Thereby, the biochip is incorporated in the platform and the U-shaped microfluidic channel is aligned with the sensors column and sealed using a pressure platform, which consists of a PCB holder and the pressure element where the PDMS channel fits in (Figure 1-3).

1.1.2 Polymerase Chain Reaction

PCR technology, which was introduced by Mullis in 1985, is a powerful research tool for DNA amplification and has become the method of choice to exponentially amplify specific DNA sequences of interest in a sample through repetitive temperature cycling[11,12,18]. A typical PCR process consists of three main steps conducted at different optimal reaction temperatures, such as, heating up the sample to 95°C for denaturation of the double-stranded DNA (dsDNA) providing single-stranded DNA (ssDNA) for primer annealing; cooling down to annealing temperature (50°C to 70°C) to renature the specific primers with the ssDNA template and finally increasing the temperature to 72°C-74°C for enzymatic extension of the primers with thermostable DNA polymerase, such as Taq polymerase (elongation step). Ensuring repeated thermal cycling, typically 20-40 cycles, an exponential increase in the number of copies of a specific DNA sequence relative to the original DNA template is successfully achieved. Recently, several studies have emerged in this biomedical research and there has been increasing demand for the development of POC platforms combining the integration of PCR technology [4,19-21].

2 Configuration PCR chip

Materials optimization for PCR chip microfabrication process is mandatory in order to ensure temperature uniformity, to improve temperature heating and cooling ramp times and biocompatibility required for the PCR reaction. Microfabricated PCR chips and thermocyclers have generally been fabricated using the three most popular materials, silicon (Si), glass and polymers. Initially, in this project, a Si-based substrate was chosen for the biochip microfabrication process, presenting several advantages and good thermal characteristics. However, the high thermal conductivity of Si makes it difficult to maintain the zones available for fluid with uniform temperature due to its lateral heat conduction. This disadvantage induces a high dissipation of heat by Si instead of promoting the heat transfer to the fluid ensuring a rapid PCR cycling. In order to overcome these disadvantages, the glass was chosen as substrate in the PCR chip microfabrication process. Since, its thermal conductivity is lower than that of Si, glass was presented as a suitable material due to its electrical

insulating properties and ability to establish uniform temperature within a confined area while limiting lateral heat conduction. Thus, using a glass substrate the heat transfer to the PCR sample being amplified was ensured.

2.1 Microfabrication Process Optimization

During the microfabrication process of biochip following the run sheet designed by Filipe Cardoso and Verónica Martins[22], non desired results were observed at Al lift-off step (edge roughness) and when the fluid tests were performed (Al pilling). With aim to overcome these problems, the photoresist (PR) profile study and the passivation layer optimization was performed.

In the PR profile study several variables, such as pre-development and exposure energy were evaluated. This study consisted in a simplified microfabrication process, which involved only a lithography step varying the specific parameters, and 3000Å Al layer deposition and the consequent the Al lift-off. In this process three samples were submitted to different conditions, pre-development during different specific times (0, 30 and 60sec) and different exposure energy (from 75% to 100%).

The passivation layer optimization comprises the evaluation of all oxides existing at INESC MN, specifically SiO_2 (Alcatel), Al_2O_3 (UHVII), Al_2O_3 (Nordiko) 3600 with different deposition angles, SiO_2 and SiN (Electrotech) (Figure 2-1), and oxide selection that presents optimal characteristics as passivation layer, in order to ensure a uniform insulation of biochip, which is fundamental for proper biological assay performance. This study consisted in a simplified microfabrication process that involves three lithography steps, and the deposition of two metallization layers intercalated with a passivation layer. The evaluation of several variables such as oxide breakdown voltage, metal overlay, metal resistivity, scanning electron microscope (SEM) analysis and tests with fluids was performed for each oxide.

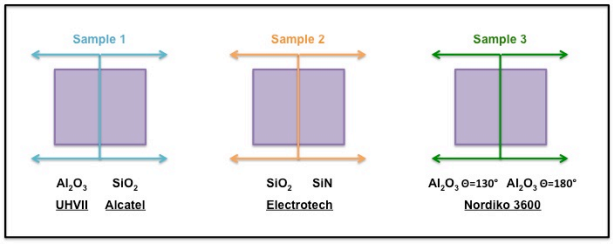

Figure 2-1: Schematic of oxide distribution in three pieces of 1-inch silicon wafer with Al_2O_3 500Å deposited at Nordiko 3600

The oxide with optimal features as passivation layer was selected taking into account the results of different fundamental tests. In this paper, only the fluid test results are shown, since it is one of the most important tests accomplished, in order to prevent the corrosion of biochip surface during the performing of PCR reaction on chip. Fluid test consisted in the evaluation of oxide behaviour in contact with a buffer solution, verifying if occurs or not the corrosion of passivation and contacts layers.

For this, one sample of each different oxide was exposed to ultraviolet light/ozone plasma for 15min inside an UVO cleaner machine (Jelight, USA) in order to minimize the contamination risk when biological assays are performed and to provide a more hydrophilic surface, increasing the number of –OH groups on the surface. For the fluidic tests, a DC power supply source was used. A 150mA current was applied in the current line. After that, 5μl or 10μl of phosphate buffer (PB), 0.1M, pH 7.4 and 0.02% (v/v) tween20, solution (depending of surface hydrophilicity) were dispensed on top of current line and current variation was registered during the process time. If the oxide was not disrupted after 1hour and 30minutes with a PB droplet on top then a stronger saline solution, phosphate buffer saline, 0.1 M and pH 7.2 (PBS) was dispensed during 1hour if possible. In Figure 2-2 are showed the fluid test results performed in samples exposed to UVO cleaner. Fluid tests were not performed in samples covered with SiO_2 (Alcatel) and Al_2O_3 (UHVII) that were submitted to UVO cleaner, since the UVO cleaner process increased the surface hydrophilicity and the droplet of PB was spread for all over the

surface, entering in contact with the pads, where were placed the electrical probes.

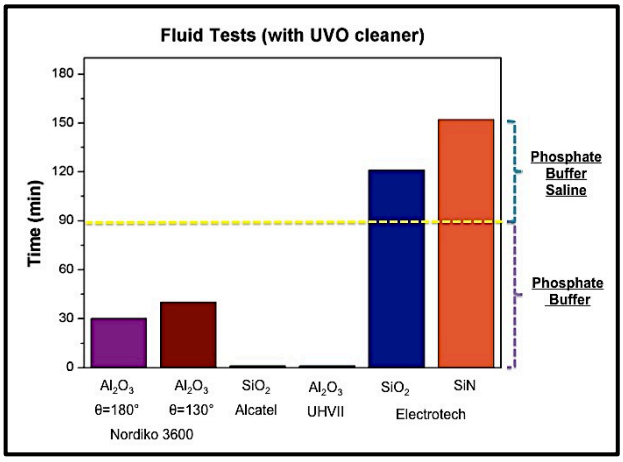

Figure 2-2: Samples performance (exposed to UVO cleaner) in contact with PB during 90 minutes and with PBS during 60 minutes.

Sample with Al_2O_3 deposited in Nordiko 3600 did not present good results, since the oxide disruption was achieved before 90 minutes. Samples covered with oxides deposited by CVD showed the best results. For both samples, SiO_2 and SiN were not disrupted during the 90 minutes in contact with PB. Then, a droplet of PBS was dispensed on the current line and the SiO_2 was disrupted after 30 minutes and the SiN after 90 minutes, accomplishing the goal of fluid test successfully. Comparing all the information obtained in optimizations tests, it can be concluded that the SiN shows the essential features and therefore it was selected as the optimal passivation layer, enabling the PCR on chip performance.

3 Temperature sensors characterization

MR sensors were calibrated as temperature sensors, which were used to detect temperature distributions while integrated current lines were used as local heating elements (Figure 3-1). For the sensors calibration and thermal parameters study, some parameters such as, a current DC value of 1mA, which was used to bias the sensor, a field DC of 50Oe ensuring the sensor saturation were defined. The sensors saturation was crucial in order to assure that any observed variation was due to the temperature and it was not influenced by any magnetic contribution. The heating procedure consisted on applying of a specific current value in the current line that consequently produces a resistance variation of MR sensors. This resistance variation can be transduced in a temperature variation. Then, inducting different current values in the current line will translate into different temperature variations, specifically 95ºC, 58ºC to 68Cº and 72ºC to 74ºC.

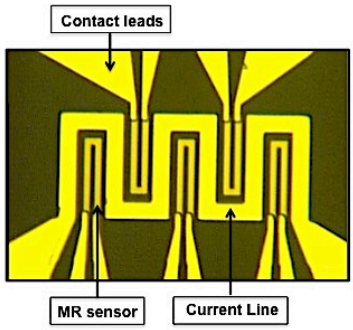

Figure 3-1: Representation of MR sensors surrounded by current line. MR sensors were used to detect the temperature and current line was used as the heating element.

3.1 MR Sensors Calibration

Simplified Equation 3-1 describes the correlation between the resistance value R of a resistor and temperature difference:

$$\boldsymbol{R = R_0\,(1 + \alpha \Delta T)} \tag{3-1}$$

where R_0 is the resistor value at room temperature, α is the material temperature coefficient of resistance (TCR) and ΔT is the temperature variation.

Moreover, the factor α (TCR) is given by ratio of resistance variation (ΔR) to temperature variation (ΔT) during a set period of time.

$$\alpha = \frac{\Delta \boldsymbol{R}}{\Delta \boldsymbol{T}} = \frac{\boldsymbol{Rmax - Rmin}}{\boldsymbol{Tmax - Tmin}} \tag{3-2}$$

where ΔR is resistance variation and ΔT is temperature variation.

In the temperature sensors calibration, three deionized (DI) water samples at different temperatures, 100ºC, 8ºC and 22ºC (room temperature (RT)) were used. The calibration of

sensors consisted in heating up and cooling down two DI water samples at specific temperatures and in the evaluation of the resistance variation for each temperature. The procedure used to calibrate the sensors consisted in the biochip introduction in the platform and the dispensing of a 10µl droplet of DI water at RT on its top. The second step was the removal and substitution of this droplet by a 10µl droplet of DI water at 100ºC. For DI water sample at 8ºC, the same method was used. The process of sensor calibration was repeated several times in order to obtain a statistic value.

The required values to estimate TCR factor correspond to maximal and minimal average value of the resistance obtained for maximal and minimal temperature (Figure 3-2 and 3-3). In Figure 3-2, the maximal average value of resistance corresponding to temperature equal to 100ºC should have been used. However, this value was not considered rigorous for this calibration. Then, the resistance average value, 916Ω ± 0.0002Ω, corresponding to RT, 22ºC (represented by green colour) was used.

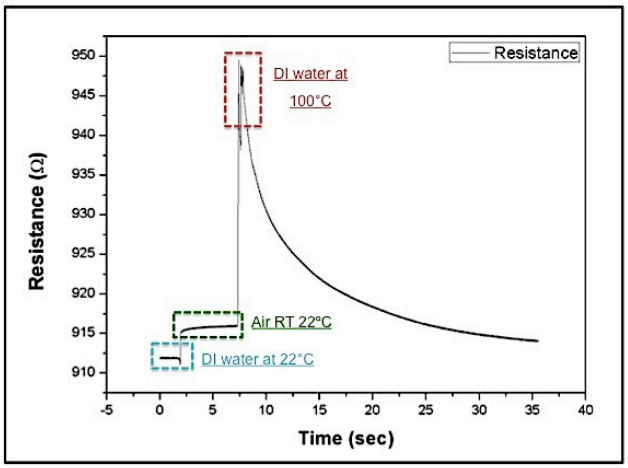

Figure 3-2: Calibration sensor: Blue square: Sensor voltage when a DI water droplet of 10µl at RT was dispensed on biochip top; Green square: Sensor voltage at RT, when the droplet DI water was removed; Red square: Sensor voltage with a 10µl droplet DI water at 100ºC on top of the biochip.

On the other hand, the resistance average value, 902Ω ± 0.0004Ω, correspondent to minimal temperature, 8ºC (presented by orange colour in Figure 3-3) was obtained.

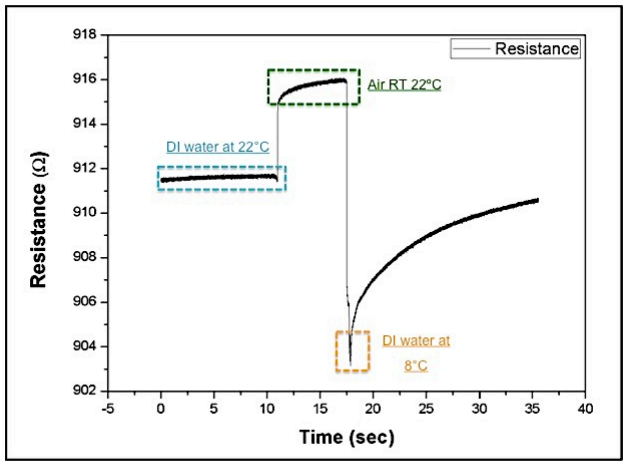

Figure 3-3: Calibration sensor: Blue square: Sensor voltage when a DI water droplet of 10µl at RT was dispensed on biochip top; Green square: Sensor voltage at RT, when the droplet DI water was removed; Orange square: Sensor voltage with a 10µl droplet DI water at 8ºC on top of the biochip

Therefore, considering the Equation 3-2, the TCR was estimated around 1.053Ω/ºC ± 0.08 Ω/ºC. Thus, using the Equation 3-1 it is possible to convert a resistance variation into a temperature variation.

Using a pulse width modulation, several heating curves were performed in order to study the increase of temperature variation with the rise of the current value and the duty cycle percentage. For this study, 10µl of PB solution was injected into the microfluidic channel placed on top of the biochip. Moreover, current values between 10mA and 60mA were applied in the current line, and different percentages of duty cycles (percentage of time in which the system was in active operation mode), between 0% and 100%, were used in different times of data acquisition. The Figure 3-4 shows the increasing of temperature variation for a constant current value, when the duty cycle percentage was also increased. Using 20%, 40%, 60%, 80% and 100% duty cycle was obtained a ΔT corresponding to 11ºC, 25ºC, 40ºC, 55ºC and 73ºC, respectively. Knowing that these measurements were performed at RT of 22ºC, using a current of 60mA and the 100% of duty cycle, the maximal temperature required for PCR cycle (95ºC) was achieved.

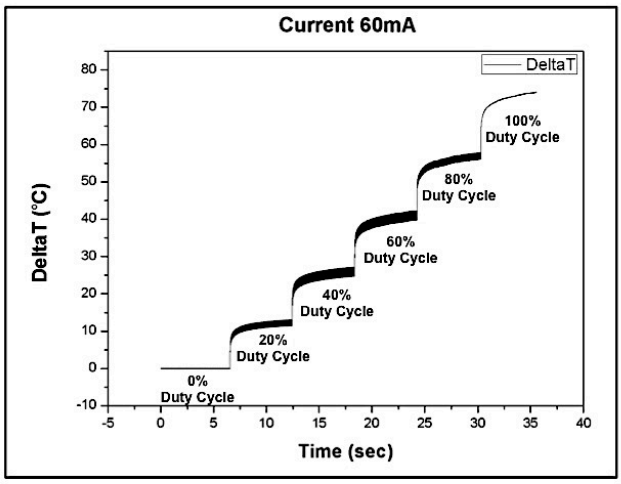

Figure 3-4: Temperature variation when a current of 60mA was applied in the current line with respective different percentages of duty cycle.

3.2 Thermal Parameters

The thermal behaviour of any system is described by the differential heat balance equation, which is presented by the following equation:

$$H\frac{dT}{dt} + G\Delta T = \Delta P \tag{3-3}$$

where H is the thermal capacitance, G is the thermal conductance, ΔT is the temperature change, t is time and ΔP represents the dissipated power change within the system.

Solving the Equation 3-3, which gives ΔT following time dependence, the Equation 3-4 was obtained. Then, considering a non linear fitting based on the Equation 3-4, the thermal parameters can be estimated in detail.

$$\frac{\Delta P}{G}\left(1 - e^{-t/\tau}\right) = \Delta T \tag{3-4}$$

where G is the thermal conductance, ΔP is the dissipated power change within the system, t is time and τ represents thermal time constant of the system.

Thermal conductance parameter

The thermal conductance is the property of a material to conduct heat, which occurs at a higher rate across materials of high thermal conductivity than across materials of low thermal conductivity. In order to study the thermal conductance a 10µl droplet of PB was dispensed on top of biochip, and different current values (from 10mA until 60mA) were applied in current line (Figure 3-1) using different percentages of duty cycle (0% until to 100%).

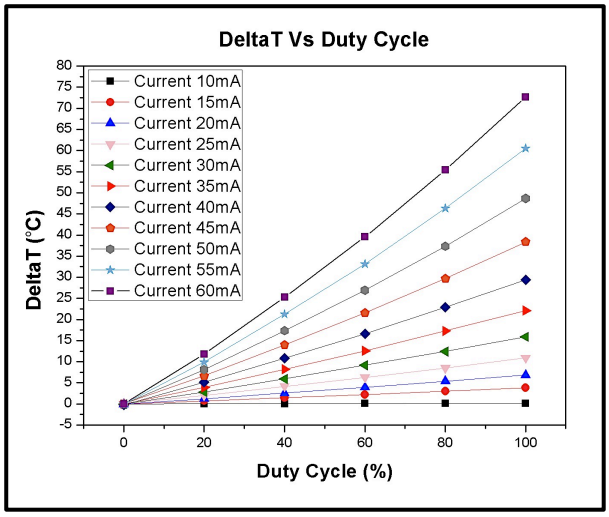

Figure 3-5: Temperature variation in function of different percentage of duty cycle for different current values applied in current line.

Regarding the Figure 3-5 can be observed that the temperature variation increases linearly with percentage of duty cycle. The most satisfactory case was obtained when a current value of 60mA was applied in current line, in which a ΔT of 73ºC was accomplished ideally.

Moreover, the instantaneous electric power, which represents the rate of energy converted from the electrical energy of the moving charged to heat, was also calculated by using the product between applied voltage and electric current on a resistor in a DC circuit. In order to obtain the Figure 3-6, it was necessary to calculate the power for all different current values with the corresponding percentage of duty cycle. Through this relation it was possible to determine the power and current value required to achieve the specific temperature. Considering the Equation 3-4, it was possible to evaluate that when time tends to infinity, the thermal conductance is given by the ratio of system power to temperature variation.

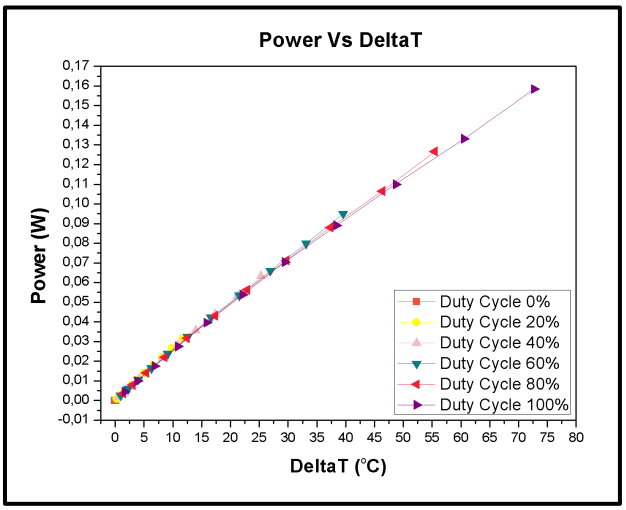

Figure 3-6: Representation of power and percentage of duty cycle applied to different current values required in order to obtain a specific temperature variation. The current line resistance was 44Ω.

Then, a linear fit of power was performed, as shown in Figure 3-7, using a specific tool of fitting available in OriginPro 8, a data analysis and graphic software application. Analysing the Figure 3-7, can be verified that the thermal conductance parameter was estimated around 2.2mW/ºC

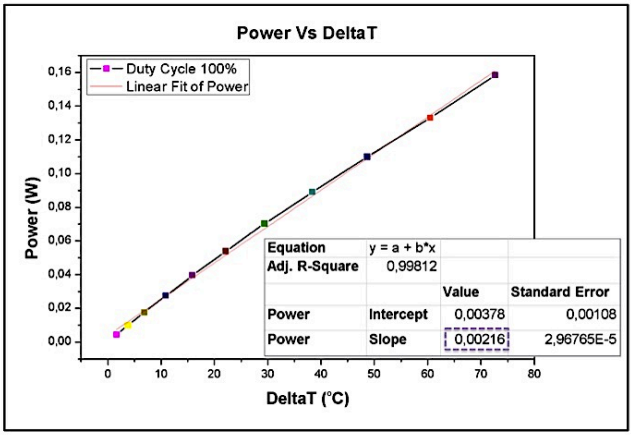

Figure 3-7: Representation of a linear fit of power when different current values were applied during the total acquisition time (100% duty cycle).

Thermal capacitance parameter

The thermal capacitance parameter is defined as the physical measurement that shows the amount of heat required to change the temperature of an object. The technique used to estimate the thermal capacitance was based on applying a maximal current value of 60mA in the current line, in which different percentages of duty cycle (0% - 100%) were applied during a maximal pulse duration imposed by the system that was equal to 8.8ms. The sampling frequency was 3000Hz and the total time of data acquisition was 6s. The data handling consisted in performing a non linear fit, following the Equation 3-5 and using the OriginPro 8 software.

$$y = (1 - e^{((-x \times G/H)}) \frac{\Delta P}{G} \quad (3\text{-}5)$$

where y and x variables correspond to the, temperature variation and acquisition time, respectively. G and H represent the thermal conductance and capacitance parameters that were estimated. ΔP corresponds to the power variation, the fixed parameter.

Regarding the information of the Figure 3-8 it is possible to evaluate the two thermal parameters. The thermal conductance, previously calculated by the first approach (2.2mW/ºC), was estimated at a similar value 2.5mW/ºC. The thermal capacitance value was estimated around 3.3µJ/ºC.

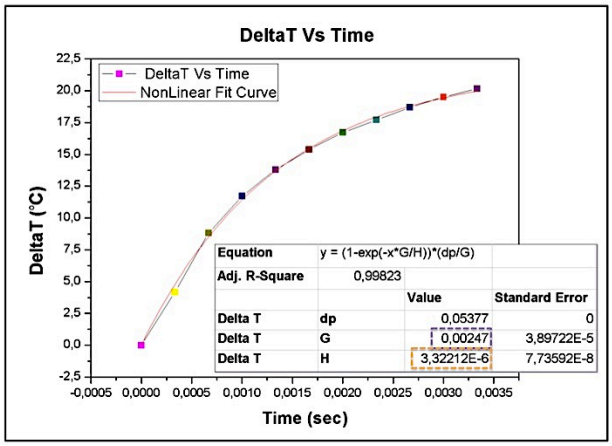

Figure 3-8: Thermal parameters estimation, H equal to 3.3µJ/ºC and G equal to 2.5mW/ºC. Non linear fit curve in which a current value of 60mA, duty cycle of 40%.

Thermal time constant

Thermal time constant is a feature of the thermal system, used when a system have a uniform rate of heating and cooling. This constant was calculated by direct ratio of thermal capacitance value to thermal conductance value following the Equation 3-6, which was evaluated in 1.151ms.

$$\tau = \frac{H}{G} \left[\frac{mJ/℃}{mW/℃}\right][s]$$

(3-6)

where H is the thermal capacitance and G is the thermal conductance.

Table 3-1 resumes the thermal and electrical parameters measured and estimated for PCR system in order to perform PCR cycles.

Table 3-1: Electrical and thermal parameters of the PCR system. All values were measured at an ambient temperature of 22ºC.

Electrical and Thermal Parameters	
Sensor Resistance	916Ω
Current Line Resistance	44Ω
Sensor TCR	1.053Ω/°C
Thermal Conductance	2.2 mW/°C
Thermal Capacitance	3.3µJ/°C
Thermal Time Constant	1.151ms

The thermal parameters estimation presented lower values than that obtained by Neuzil and its co-workers[11]. These results can be explained by different geometry of PCR system, substrate material and DNA sample volume used. Thermal conductance value can be explicated taking into account that the material selected as substrate in our PCR on chip system was glass, which presents a lower thermal conductivity than Si substrate, providing thermal insulation instead of heat dissipation. The low thermal capacitance parameter can be understood, since the DNA sample volume is only 10µl instead of 1mL, then the thermal capacitance represents shows the amount of heat required to change the temperature.

4 Polymerase Chain Reaction on chip

In this work, a particular cell free DNA fragment of 115bp, from ALU repeated sequence, was targeted for amplification. The template used for amplification reaction consisted in the genomic DNA extracted from cultured Human Embryonic Kidney (HEK) 293T cells. For ALU115 fragment generation, a primer set was synthesized and purchased from StabVida, Portugal. A PCR mixture was prepared following a protocol used in a previous work [23]. The real time PCR (rt-PCR) was always performed a few minutes before PCR on chip, in order to evaluate if any component of solution or condition (temperature or cycle time) could inhibit the amplification DNA. A typical rt-PCR thermocycle consists in 25 cycles for 10 sec at 95ºC, 4 sec at 65ºC and 4 sec at 72ºC. The initial step, 10 min at 95ºC was achieved in a conventional thermocycler. The PCR on chip cycle consisted of an additional step of 30sec at 95ºC in first cycle (to ensure that 95ºC was achieved), followed by 25 cycles for each 0.5µl of PCR mixture, 13sec at 95ºC (denaturation step), 8sec at 65ºC (annealing step) and 5sec at 72ºC (extension step). Then, three different percentage of duty cycle were used such as, 97%, 68% and 74% in order to achieve the three different temperatures, 95ºC, 68ºC and 72ºC respectively.

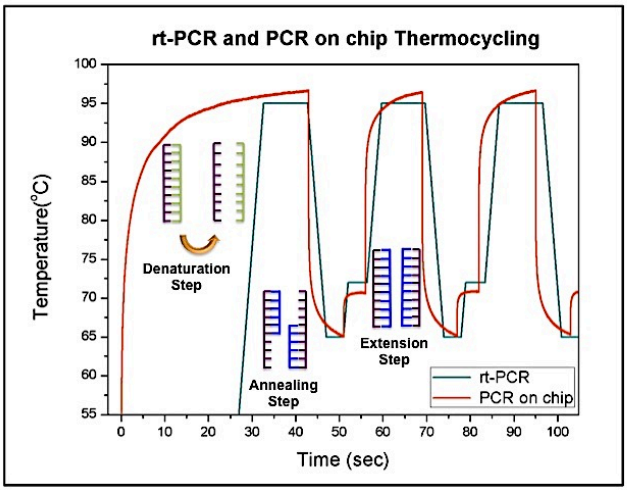

Figure 4-1: Analysis of the three first PCR cycles in detail. Representation of three crucial steps to PCR performing, 13 sec at 95ºC (denaturation step), 4 sec at 65ºC (annealing step) and 4 sec at 72ºC (extension step). The different temperatures were similarly achieved at the identical cycle times.

In Figure 4-1 it was possible to evaluate an overlap between the two different amplification techniques being used, in which the cycle times were very similar but not totally equal. Therefore, the Figure 4-1 reveals an important result for PCR on chip performing, since the thermal control achieved for PCR on chip, controlled by PWM, was very rigorous and crucial.

Agarose gel (2%) was used to analyse the results of rt-PCR and PCR on chip products (Figure 4-2).

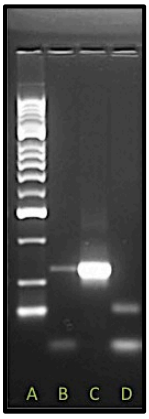

Figure 4-2: Analysis of PCR products in an agorose (2%) gel electrophoresis: A – HypperLadder II Bioline (ranging from 50bp to 2000bp); B – Negative control sample; C – rt-PCr products sample; D – PCR on chip products sample.

In A gel pad is represented the HyperLadder II Bioline marker used to quantify the sample bands and identify the DNA fragments molecular weigh. The B corresponds to the negative control, in which should not present amplification in any cycle or time. However, the fragment with 115bp observed can be understood as a contamination, since the sequence (ALU115 fragment) exists in a large quantity in the human genome. The C pad corresponds to the rt-PCR products, represented by a fragment with 115bp. This would also be the result also expected for the PCR on chip sample. However, in D pad was verified a fragment with a corresponding size of about 75bp. Although, the PCR on chip results demonstrate a non specific DNA amplification, this can be considered a crucial and promising result for PCR on chip research.

5 Conclusion and Future Work

The results obtained were crucial for passivation later optimization in order to avoid the corrosion during PCR on chip assay. Along this paper a big step was accomplished on the integration of PCR in a MR biochip. However some modifications and improvements can be suggested in order to obtain a specific DNA amplification such as, using an enzyme with a lower activation time, from 10 min to 1 min, the entire amplification process can be accomplished inside the MR platform, avoiding the possibility of primers dimers formation. The rigorous thermal control provided by proportional integral derivative algorithm implementation would be crucial to ensure that the three specific temperatures would be achieved, specially the annealing temperature that should not be undershoot in order to prevent false annealing primers and consequently decreasing the specificity of the PCR. The surface passivation could be achieved by blocking the surface with passivation agents, e.g. bovine serum albumin (BSA) to reduce the undesired adsorption of enzyme and DNA to channel wall and surface.

References

[1] W. G. Lee, Y.G. Kim, B.G. Chung, U, Demirci, and A. Khademhosseini, *Advanced drug delivery reviews*, 2010, **62**, 449-457.
[2] P.Yager, G.J. Domingo and J.Gerdes, *Annual review of biomedical engineering*, 2008, **10**, 107-144.
[3] D.C.Hay Burgess, J. Wasserman and C.A. Dahl, *Nature*, 2006, **444**, 1-2.
[4] M.G.Roper, C.J.Easley and J.P. Landers and *Analytical chemistry*, 2005, **77**, 3887-3893.
[5] P.J.Obeid, T.K.Cristopoulos, H.J. Crabtree and C.J. Backhouse, *Analytical chemistry*, 2003, **75**, 288-295.
[6] C. D. Chin, V. Linder and S. K. Sia, *Lab on a chip* **7**(1), 41-57 (2007).
[7] C. Zhang and D. Xing, *Nucleic acids research* **35**(13), 4223-4237 (2007).
[8] Q.Xiang, B.Xu and D. Li, Biomed Microdevices **9**, 443-449 (2007)
[9] I. Schneegass, R. Brautigam and J. M. Kohler, *Lab on a chip* **1**(1), 42-49 (2001)
[10] Z. Guttenberg, H.Muller, H. Habermuller, A.Geisbauer, J. Pipper, J.Felbel, M.Kielpinski, J.Scriba and A.Wixforth, *Lab on a chip* **5**, 308-317 (2005).
[11] P. Neuzil, J. Pipper and T.M. Hsieh, *Molecular bioSystems*, 2006, **2**, 292-298.
[12] M. Hashimoto, P.C. Chen, M.W. Mitchell, D.E. Nikitopoulos, S.A. Soper and M.C. Murphy, *Lab on a chip*, 2004, **4**, 638-645.
[13] J.Germano, V.C. Martins, F.A. Cardoso, T.M. Almeida, L.Sousa, P.P. Freitas and M.S.Piedade, *Sensors*, 2009, **9**, 4119-4137.
[14] D.L.Graham, H.A. Ferreira, and P.P. Freitas, *Trends in biotechnology*, 2004, **22**, 455-462.
[15] R.L.Millen, T. Kawaguchi, M.C.Granger, M.D. Porter and M.Tondra, *Analytical chemistry*, 2005, **77**, 6581-6587.
[16] H.A. Ferreira, N. Feliciano, D.L.Graham, L.A. Clarke, M.D.Amaral and P.P. Freitas, *Applied Physics Letters*, 2005, **87**, 013901.
[17] V.C. Martins, J. Germano, F.A. Cardoso, J. Loureiro, S. Cardoso, L. Sousa, M. Piedade, L.P. Fonseca and P.P. Freitas, *Journal of Magnetism and Magnetic Materials*, 2010, **322**, 1655-1663.
[18] D.S. Lee and C.S. Chen, *Biosensors & bioelectronics*, 2008, **23**, 971-979.
[19] P. Neuzil, C. Zhang, J. Pipper, S. Oh and L, Zhuo, *Nucleic acids research*, 2006, **34**, e77.
[20] M.U. Koop, A.J. Mello, and A, Manz, *Science*, 1998, **280**, 1046-1048.
[21] S.H. Lee, S.W. Kim, J.Y. Kang and C.H. Ahn, *Lab on a chip*, 2010, **8**, 2121-2127.
[22] F.A. Cardoso, PhD, Instituto Superior Técnico, 2010.
[23] T. Dias, Master, Instituto Superior Técnico, 2011.